www.czasopisma.pan.pl PAN www.journals.pan.pl
POLSKA AKADEMIA NAUK

JOURNAL OF WATER AND LAND DEVELOPMENT
e-ISSN 2083-4535

Polish Academy of Sciences (PAN), Committee on Agronomic Sciences
Institute of Technology and Life Sciences (ITP)

JOURNAL OF WATER AND LAND DEVELOPMENT
2021, No. 48 (I–III): 197–204; https://doi.org/10.24425/jwld.2021.136162

Available (PDF): https://www.itp.edu.pl/JWLD; http://journals.pan.pl/jwld

Received 25.05.2020
Reviewed 01.06.2020
Accepted 22.10.2020

The kinetics, thermodynamics and equilibrium study of nickel and lead uptake using corn residues as adsorbent

Candelaria TEJADA-TOVAR, Ángel VILLABONA-ORTÍZ, Angel Darío GONZALEZ-DELGADO ✉

University of Cartagena, Avenida del Consulado Calle 30 No. 48-152, Cartagena, Bolívar, Colombia

For citation: Tejada-Tovar C., Villabona-Ortíz Á., Gonzalez-Delgado A.D. 2021. The kinetics, thermodynamics and equilibrium study of nickel and lead uptake using corn residues as adsorbent. Journal of Water and Land Development. No. 48 (I–III) p. 197–204. DOI 10.24425/jwld.2021.136162.

Abstract

Agricultural residues rich in lignocellulosic biomass are low-cost and sustainable adsorbents widely used in water treatment. In the present research, thermodynamics, kinetics, and equilibrium of nickel(II) and lead(II) ion biosorption were studied using a corncob (*Zea mays*). The experiments were performed in a batch system evaluating the effect of temperature and dose of adsorbent. Langmuir and Freundlich isotherms were used to study the equilibrium. Thermodynamic and kinetic parameters were determined using kinetic models (pseudo-first order, pseudo-second order, Elovich). Biosorbent characteristics were studied by Fourier-transform infrared spectroscopy, Scanning Electron Microscopy and Energy-dispersive X-ray spectroscopy. It was found that the hydroxyl, carboxyl, and phenolic groups are the major contributors to the removal process. Besides, Pb(II) ions form micro-complexes on the surface of the biomaterial while Ni(II) ions form bonds with active centers. It was found that the highest Ni(II) removal yields were achieved at 0.02 g of adsorbent and 70°C, while the highest Pb(II) removal yields were achieved at 0.003 g and 55°C. A maximum Ni(II) adsorption capacity of 3.52 mg·g^{-1} (86%) and 13.32 mg·g^{-1} (94.3%) for Pb(II) was obtained in 250 and 330 min, respectively. Pseudo-first order and pseudo-second order models best fit experimental data, and Langmuir and Freundlich models well describe the isotherm of the process. Thermodynamic parameters (ΔH_0, ΔG_0, ΔS_0) suggest that the adsorption process of both cations is exothermic, irreversible, and not spontaneous.

Key words: *adsorption, corn wastes, heavy metals, kinetics, thermodynamics*

INTRODUCTION

Heavy metal ions from human activity (industry, agriculture, tanneries, fertilizer manufacturing, batteries, and mining waste disposal) pose a serious environmental problem, since residual highly contaminated effluents are discharged into the environment reaching concentrations of heavy metals above permissible values [GAŁCZYŃSKA *et al*. 2019]. Rapid industrial and urban developments have put significant pressure on natural resources. Since water is vital to life, it is a scarce resource worth fighting for [LIU *et al*. 2009].

Water ecosystems are affected by the presence of heavy metals, in particular their resistance to degradation, persistence, and tendency to bioaccumulate in living organisms [RAVAL *et al*. 2016]. Lead is harmful to vital organs and systems, and its toxicity triggers enzymatic inhibition [SIREGAR *et al*. 2020]. Moreover, nickel can cause dermatitis, genotoxic effect on lungs, liver, kidneys, and brain, inhibition of enzymatic action, alteration of protein function, calcium deficiency in bones, DNA damage, cancer, etc. [SINGH, SHUKLA 2017].

Nowadays, several options are available to remove metal ions from wastewater, such as coagulation-flocculation, membrane filtration, flotation, chemical precipitation,

and electrochemical precipitation [HERNÁNDEZ RODIGUEZ *et al*. 2018]. However, some of these methods produce large volumes of sludge, which increases the risk of metal ion leaching. Therefore, easy-to-operate, low cost and safe systems are needed to remove metal ions [YI *et al*. 2017]. Among available techniques, adsorption seems to be an attractive method to remove heavy metals from a solution [VALENCIA *et al*. 2019]. There is a growing interest in the development of adsorbents that meet requirements. These include an open-pore structure for fast kinetics, accessible adsorption sites, surface properties suitable for high adsorption capacity, simple synthesis, and low cost [DAI *et al*. 2018]. Heavy metals can also be immobilized through precipitation [SHI *et al*. 2019].

Biomasses have gain special interest due to their availability and potential characteristics [OUHIMMOU *et al*. 2019]. Biosorbents derived from biomass contribute to sustainable development, taking into account that the traditional supply chain has been replaced by a more environmentally friendly chain that ensures economic development, as well as environmental and social improvement [BABAZADEH *et al*. 2017]. Environmental uses of biosorbents depend mainly on their interaction with heavy metals. For instance, in water treatment, we may expect the presence of multiple contaminants in a solution and possible reuse of the adsorbent [SHEN *et al*. 2017]. Consequently, for their practical applications, it is crucial to identify mechanisms of interaction between the adsorbent and heavy metals.

This research attempted to evaluate the use of the corncob as an adsorbent, its thermodynamics, kinetics, and the balance of Ni(II) and Pb(II) adsorption. The bioadsorbent was characterized by the Fourier-transform infrared spectroscopy (FT-IR), Scanning Electron Microscopy (SEM), and Energy-dispersive X-ray spectroscopy (EDS), identifying functional groups involved in metal removal, morphology, composition, and mechanisms of metal removal. Adsorption tests were performed in a batch system, followed by the evaluation of temperature and adsorbent dose influence on the process.

MATERIAL AND METHODS

MATERIALS AND EQUIPMENT

Lead(II) nitrate ($Pb(NO_3)_2$) and nickel (II) sulphate ($NiSO_4$) provided by Sigma Aldrich were used for the experimental development. Shaker incubator IN-666 from Gemmy industrial brand, Spectrophotometer IR Shimadzu IRAinfinity-1S, Electron Scanning Microscope JEOL Ltd. model JSM 6490-LV. All reagents used were of analytical grade.

EXPERIMENTAL DESIGN

The design of continuous factor experiments on the central composite response surface (star) was used, as shown in Table 1 and developed with Statgraphics Centurion XVI.II.

Table 1. Experimental design

Independent variables	Unit	Range and level				
		−α	−1	0	+1	+α
Adsorbent amount	g	0.0034	0.02	0.06	0.1	0.1166
Temperature	°C	33.79	40	55	70	76.21

Source: own elaboration.

ADSORBENT PREPARATION AND CHARACTERIZATION

The corncob was collected fresh, washed and dried in an oven at 70°C for 24 hours until it formed a dry mass. Then, a particle size of the lignocellulosic material was reduced using a conventional grounder and sieve-meshed to 0.355 mm [ABDUL-HAMEED, AL JUBOURY 2020]. The resulting material was characterized before and after the adsorption process by SEM, EDS, and FTIR analyses to determine its morphology, composition, and functional groups present that could be involved in the removal process [MANIRETHAN *et al*. 2019].

ADSORPTION TESTING

For the adsorption tests, synthetic solutions of lead and nickel were prepared in concentrations of 29.35 $mg \cdot dm^{-3}$, using lead(II) nitrate and nickel(II) sulphate as reagents. The lead solution was adjusted to pH 5 and the nickel solution to pH 6, using NaOH and 1 M HCl. Solutions were mixed with the biomass at 200 rpm for 24 h, following the experimental design in Table 1. Optimal adsorption conditions were determined based on the results obtained [MANJULADEVI *et al*. 2018]. The final concentration at equilibrium was determined by the Atomic Absorption Spectroscopy (AA) at 232 and 217 nm for nickel and lead, respectively. Adsorption efficiency and capacity were determined by Equations (1) and (2):

$$\%R = \frac{C_0 - C_f}{C_i} 100 \quad (1)$$

$$q_e = \frac{V(C_0 - C_f)}{m}$$

Where: C_0 = the initial concentration ($mg \cdot dm^{-3}$); C_f = the final concentration ($mg \cdot dm^{-3}$); V = volume (dm^3); m = the mass of adsorbent (g); $\%R$ = the adsorption efficiency; q_e = the adsorption capacity of the adsorbent ($mg \cdot g^{-1}$).

The data statistical analysis was performed using Statgraphics Centurion XVI.II, analysis of variance (ANOVA), effect plots, standardized effect Pareto chart, to determine the incidence of evaluated variables and the percentage of lead and nickel adsorption.

KINETICS AND ADSORPTION ISOTHERMS

Under optimal conditions of temperature, particle size, and adsorbent dose that presented the highest percentage of removal for each metal and biomass, kinetic studies were performed by taking eight samples at different time intervals (0, 10, 30, 60, 180, 240, 300 and 1440 min) [ABDUL-HAMEED, AL JUBOURY 2020]. Experimental kinetic data were adjusted to the pseudo-first order, pseudo-second or-

der and Elovich models (Tab. 2) using the curve fitting tool of the Origin Pro 9® program. This helped to examine the lead and nickel adsorption with lemon peel and corncob over time and to determine the adsorption mechanism in each of these systems.

Table 2. Kinetic models of adsorption in the batch system

Model	Equation	Parameters explanation
Pseudo--first order	$q_t = q_e(1 + e^{-k_1 t})$	q_t (mmol·g^{-1}): adsorption capacity at time t q_e (mmol·g^{-1}): adsorption capacity at the equilibrium k_1 (min^{-1}): first order kinetic constant
Pseudo--second order	$q_t = \frac{t}{\frac{1}{k_2 q_e^2} + \frac{t}{q_e}}$	k_2 (g·mmol^{-1}·min^{-1}): kinetic constant of pseudo-second order and the initial adsorption rate q_e: adsorption capacity in equilibrium
Elovich	$q_t = \frac{1}{\beta}\ln(\alpha\beta) + \frac{1}{\beta}\ln t$	α (mmol·g^{-1}·min^{-1}): initial rate of adsorption β (mmol·g^{-1}): related to the surface area covered and the activation energy by chemical adsorption

Source: own elaboration.

Adsorption isotherms were developed to describe the amount of nickel and lead in the equilibrium of the sorbate between solid and liquid phases. The experiments were conducted using different concentrations of lead (20, 40, 60, and 80 ppm) and nickel (5, 10, 15, and 20 ppm), with a single sample taken at the end of 24 hours. Langmuir and Freundlich models were used to adjust the data (Tab. 3).

Table 3. Adsorption isotherm models in the batch system

Model	Equation	Parameters explanation
Langmuir	$q_e = q_{\max}\frac{K_L C_f}{1+K_L C_f}$	q_e: adsorption capacity at the equilibrium C_f: remaining heavy metal concentration in the solution. $q_{\max}$: maximum adsorption capacity K_L: ratio of the adsorption/desorption rate
Freundlich	$q = K_F C_e^{\frac{1}{n}}$	q (mg·g^{-1}): adsorption capacity C_e (mg·dm^{-3}): concentration at the equilibrium K_F (dm^3·mg^{-1}): parameter related to the affinity of the bioadsorbent for metal ions n: parameter related to adsorption intensity

Source: own elaboration.

THERMODYNAMIC PARAMETERS

A thermodynamic study was conducted to understand the nature of the Ni(II) and Pb(II) adsorption process on the corncob. For this purpose, the change in Gibbs' standard free energy ($\Delta G°$), standard enthalpy ($\Delta H°$) and standard entropy ($\Delta S°$) were calculated, according to Equations (2)–(6).

$$\Delta G° = RT \ln k_c \quad (2)$$

$$\ln k_c = \frac{-\Delta H}{R \cdot T} + \frac{\Delta S°}{R} \quad (3)$$

$$\Delta H° = -m\,R \quad (4)$$

$$\Delta S° = R\,b \quad (5)$$

$$k_c = \frac{q_e}{C_e} \quad (6)$$

Where: k_c = the equilibrium constant; q_e = the equilibrium solid phase concentration (mg·g^{-1}); C_e = the equilibrium concentration (mg·g^{-1}); R = the ideal gas constant; T = the absolute temperature (K).
$\Delta H°$ and $\Delta S°$ are determined from the slope and the y-axis intercept of ln k_c vs. T–1, respectively, following the van't Hoff graphical method.

RESULTS AND DISCUSSION

ADSORBENT CHARACTERIZATION

The corncob EDS spectrum shown in Figure 1a demonstrated that the predominant element in the biomass structure is carbon (59.62%), followed by oxygen (35.02%), due to the lignocellulosic nature of the material; the presence of materials in smaller proportion as Si, K and Sn was also found. After adsorption of Pb(II) and Ni(II) – Figures 1b and 1c, the presence of the metals on the surface of the adsorbent was evident. Meanwhile, C and O were the materials with the highest presence in the adsorbent, with a slight increase in their percentages in weight which can be attributed to the formation of links between ions and biomass.

Figure 2a presents the micrograph of the corncob before adsorption and exhibits a porous flaky irregular sur-

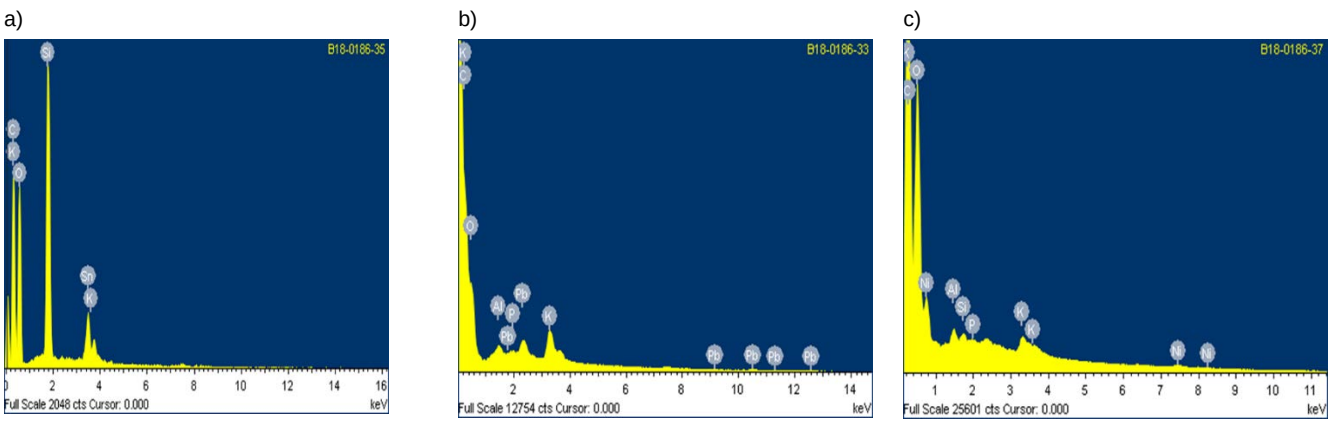

Fig. 1. Energy-dispersive X-ray spectroscopy spectrum of corncob: a) before removal of Pb(II) and Ni(II), b) after removal of Pb(II), c) after removal of Ni(II); source: own study

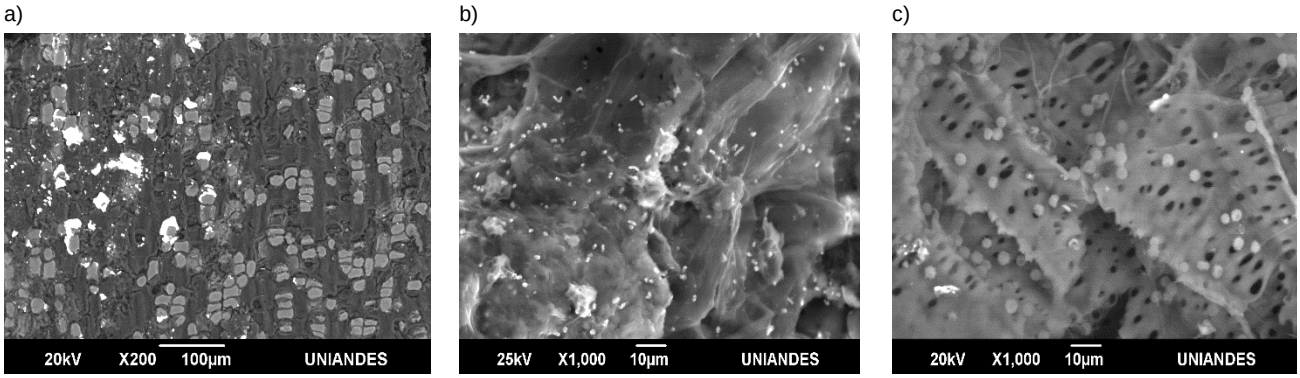

Fig. 2. Scanning electron microscope images of corncob: a) before removal of Pb(II) and Ni(II), b) after removal of Pb(II), c) after removal of Ni(II); source: own study

face, which promotes a better heterogeneous biosorption due to the large interface [PRADHAN *et al.* 2018]. From SEM microphotographs obtained after the adsorption process (Figs. 2b, c), it was observed that Pb(II) was adsorbed on the surface of the material with the ion agglomeration that is attributed to the formation of chelates by microcomplexity [TEJADA-TOVAR *et al.* 2019a]; it was found that the removal of Ni(II) in corn sludge occurs by electrostatic attraction forces between active centers and the ion.

Figure 3 illustrates the FTIR spectrum for the corncob before and after the adsorption process. The complexity of the lignocellulosic material was confirmed due to the various bands identified. Several peaks were identified at 3200–3500 cm^{-1} (OH and secondary amines), 2927.94 cm^{-1} (methoxy group), 2500 cm^{-1} (COOH), 1650 cm^{-1} (C=CC), 1000–1200 cm^{-1} (alcohols), and 950 cm^{-1} (C-N) [JOHARI *et al.* 2016]. After the metal adsorption process, changes were observed in width and amplitude of the bands: 3390 cm^{-1} (NH), 2361.19 cm^{-1} (–C≡N), 1650 cm^{-1} (C=C), 1120.66 cm^{-1} (OH), and 1156.55 cm^{-1} (sulphonamides) [ABDUL-HAMEED, AL JUBOURY 2020]; this can be explained by the formation of bonds between the Pb(II) and Ni(II) ions and the active centers of the material [TEJADA-TOVAR *et al.* 2019b].

EFFECT OF TEMPERATURE AND DOSE OF ADSORBENT

The amount of biosorbent used for adsorption studies is an important parameter which determines the potential of the biosorbent to remove metal ions at their given initial concentration [BUREVSKA *et al.* 2017]. Moreover, the influence of temperature on metal removal processes determines mechanisms that define and control the process [YIN *et al.* 2019]. The relationship between biosorbent dose, temperature, and the adsorption capacity of nickel(II) and lead(II) is shown in Table 4.

Figure 4 describes the effect of the adsorbent dose and temperature on the percentage of nickel adsorption on corn silage. It is observed that higher temperature results in lower adsorption, which is expected to be exothermic [CHERIK, LOUHAB 2018]; moreover, higher adsorbent dose results in better nickel adsorption because higher adsorbent amount increases the availability of active sites available for metal removal [IBISI, ASOLUKA 2018].

Figure 5 presents the lead adsorption efficiency depending on temperature and adsorbent dose; it is observed that the removal efficiency increases gradually with temperature and adsorbent dose, and the removal is the lowest

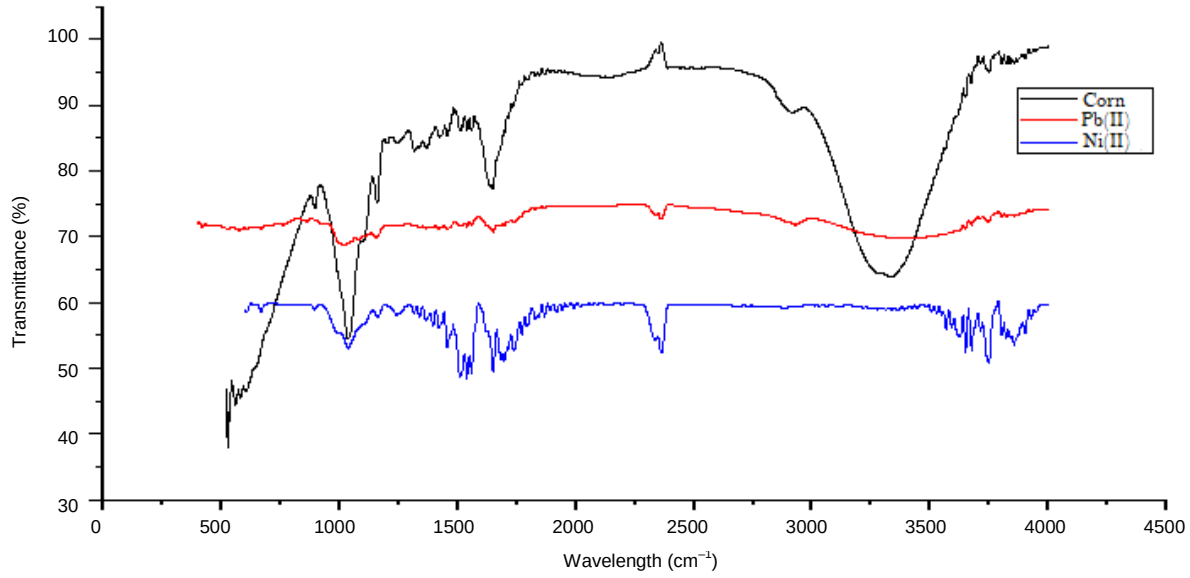

Fig. 3. The infrared spectrum of corncob before and after adsorption; source: own study

Table 4. Adsorption capacity of lead(II) and nickel(II) at different adsorbent dosage and temperature

Adsorbent amount (g)	Temperature (°C)	Adsorption capacity q (mg·g^{-1})	
		Pb(II)	Ni(II)
0.06	33.79	15.9298	3.6519
0.1	40	8.4991	1.2926
0.02	40	41.9664	10.7959
0.06	55	17.1369	3.7323
0.003	55	305.5055	61.7968
0.116	55	8.7629	1.9421
0.02	70	44.0669	8.5639
0.1	70	9.9180	1.9409
0.06	76.21	15.5909	3.2783

Source: own study.

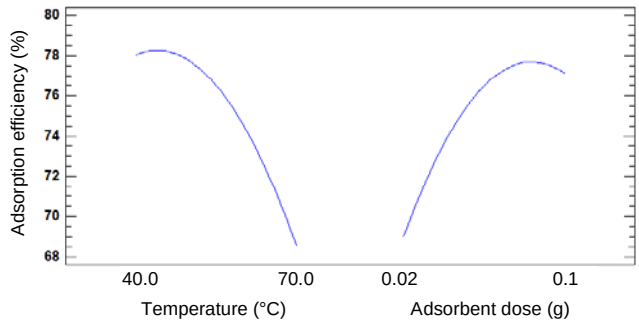

Fig. 4. Effect of temperature and adsorbent dose on nickel(II) adsorption; source: own study

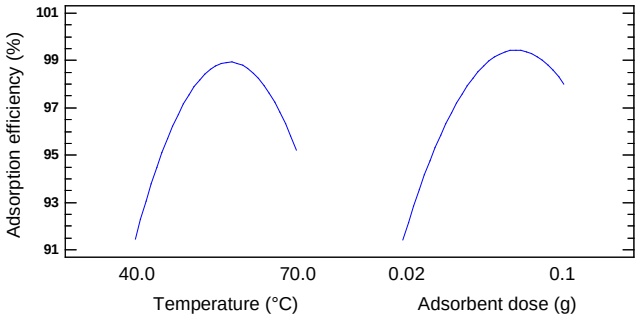

Fig. 5. Effect of temperature and dosage of adsorbent on lead(II) adsorption; source: own study

at low temperature and adsorbent dose. However, maximum adsorption occurs at the intermediate points of temperature and adsorbent dose, because temperature affects adsorption equilibrium. Higher temperatures tend to improve adsorption capacity and facilitate porous diffusion in adsorbent materials [HERNÁNDEZ RODIGUEZ *et al*. 2018].

Figure 6a presents the Pareto chart for the process of extracting nickel from corncobs; it is observed that temperature had a negative impact on the adsorption capacity of the system, while the adsorbent dose had a positive effect. Figure 6b illustrates the Pareto diagram for lead removal; it is observed that temperature and adsorbent dose, in the ranges evaluated, had no significant effect on adsorption in the system.

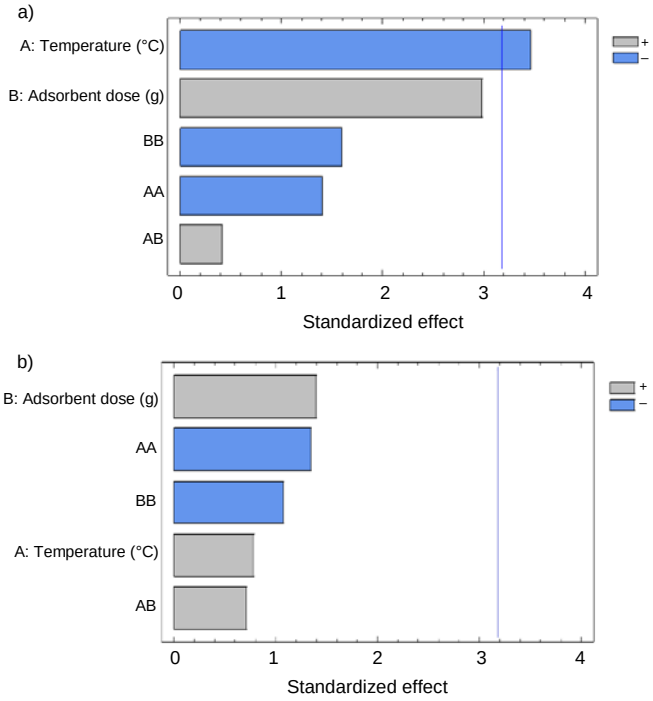

Fig. 6. Pareto diagram for the adsorption of investigated heavy metals on corncob: a) nickel, b) lead; source: own study

The analysis of variance (Tab. 5) indicates the numerical significance of independent variables within the ranges evaluated on the nickel and lead removal process with a *P*-value lower than 0.05, which corroborates the findings of the Pareto chart in Figure 6.

According to the analysis of variance (ANOVA) shown in Table 5, the statistical significance of the adjusted equation was estimated by the established variance ratio and the determination coefficients (R^2). The ANOVA regression coefficients of the model obtained with the Stat graphics Centuryon software showed that the quadratic fitted equations (Eqs. 7, 8) had statistical significance for the removal of nickel(II), as clearly seen in the value of

Table 5. Analysis of variance for lead(II) and nickel(II) adsorption

Source	Ni(II)					Pb(II)				
	sum of squares	*df*	mean square	*F* ratio	*P* value	sum of squares	*df*	mean square	*F* ratio	*P* value
A: temperature	180.5060	1	180.5060	16.70	0.0150	28.2522	1	28.2522	0.85	0.4080
B: adsorbent dosage	124.4620	1	124.4620	11.51	0.0274	80.2190	1	80.2190	2.42	0.1946
AA	49.3199	1	49.3199	4.56	0.0995	142.0030	1	142.0030	4.29	0.1072
AB	2.6050	1	2.6050	0.24	0.6492	23.2420	1	23.2420	0.70	0.4493
BB	63.3334	1	63.3334	5.86	0.0727	94.8552	1	94.8552	2.86	0.1658
Total error	43.2385	4	10.8096			132.4870	4	33.1218		

Explanations: *df* = degrees of freedom, *F* = F statistic, *P* = probability value.
Source: own study.

that the estimated value is large enough to validate a very high order of acceptability for the quadratic statistical model [BARDESTANI *et al*. 2019]. The R^2 was higher than 90% for the two metals, it showed that the variability of the adsorption could be explained by the model, with the coherence between experimental and predicted values significant for the process [KAPLAN INCE *et al*. 2017]. As a result, optimal values of the independent parameters of adsorbent dose 0.003 g and temperature 55°C were observed. Under these conditions, it was predicted that the maximum Ni(II) adsorption would be 65 mg·g^{-1} and for Pb(II) 325,553 mg·g^{-1}.

$$\text{Pb(II) adsorption} = 17.6829 + 7.7531x_1 - 5625.71x_2 - 0.0701x_1^2 - 0.284x_1x_2 + 34321.6x_2^2 \quad (7)$$

$$\text{Ni(II) adsorption} = 10.256 + 1.4445x_1 - 1210.71x_2 - 0.0139x_1^2 + 1.2001x_1x_2 + 6914.85x_2^2 \quad (8)$$

Where: x_1 = the temperature (°C); x_2 = adsorbent dosage (g).

ADSORPTION KINETICS

Figure 7 shows the experimental data that fit into to the pseudo-first order, pseudo-second order, and Elovich kinetic models used to determine steps that control the process. Based on the adjustment, it can be established that the first and second order models best describe the nickel and lead removal data with R^2 0.994 and 0.999, respectively.

Figure 7 shows that the adsorption of both ions is very fast in the initial stages of the process, and from the 60th minute, it gradually decreases until equilibrium. This suggests that the availability of active sites in the biomass has been reduced. The fitting to the pseudo-first order model establishes that the adsorption rate depends on a mechanism operating at an active site on the biomass surface [ABDUL-HAMEED, AL JUBOURY 2020]. Moreover, the pseudo-second order model states that the mechanism that the controlled adsorption is chemical, so the rate of adsorption is limited by valence forces from the exchange of electrons between the adsorbate and the adsorbent [CHEN *et al*. 2018].

Table 6 depicts the adjustment parameters of the kinetic models for the adsorption of nickel(II) and lead(II) on the corncob; it is established that the theoretical adsorption capacity (q_e) is correlated with data obtained experimentally (3.52 mg·g^{-1} for nickel and 13.32 mg·g^{-1} for lead).

Table 6. Adjusting parameters of the kinetic models of nickel(II) and lead(II) adsorption

Model	Parameter	Ni(II)	Pb(II)
Pseudo-first order	q_e (mg·g^{-1})	3.5055	13.2091
	k_1 (min^{-1})	91.64897	0.5408
	R^2	0.9994	0.9996
Pseudo-second order	q_e (mg·g^{-1})	3.5055	13.2042
	k_2 (g·mg^{-1}·min^{-1})	3.11E+13	8.5839
	R^2	0.9994	0.9996
Elovich	α (g·mg^{-1}·min^{-1})	3.653544	1.41E+43
	β (g·mg^{-1})	31.621	8.04733
	R^2	0.996	0.997

Explanations: q_e = adsorption capacity at the equilibrium, k_1 = first order kinetic constant, R^2 = determination coefficient, α = initial rate of adsorption, β = related to the surface area covered and the activation energy of chemical adsorption.
Source: own study.

ADSORPTION ISOTHERMS

Adsorption isotherms describe the concentration dependence of the degree of adsorption at a constant temperature, and the nature of the binding forces between the adsorbate and the adsorbent, such as physical or chemical forces [NASEEM *et al*. 2019]. The equilibrium data for nickel and lead have been fitted to Langmuir and Freundlich isotherm models and are presented in Figure 8, at the optimum condition of temperature, adsorbent dosage, and particle size for each metal. Table 7 shows the fitting parameters.

As shown in Figure 8 and according to parameters in Table 7, both models fitted well experimental data. However, the Freundlich's model best describe data for both heavy metal ions based on the correlation parameters (R^2). This suggests that both physical and chemical mechanisms

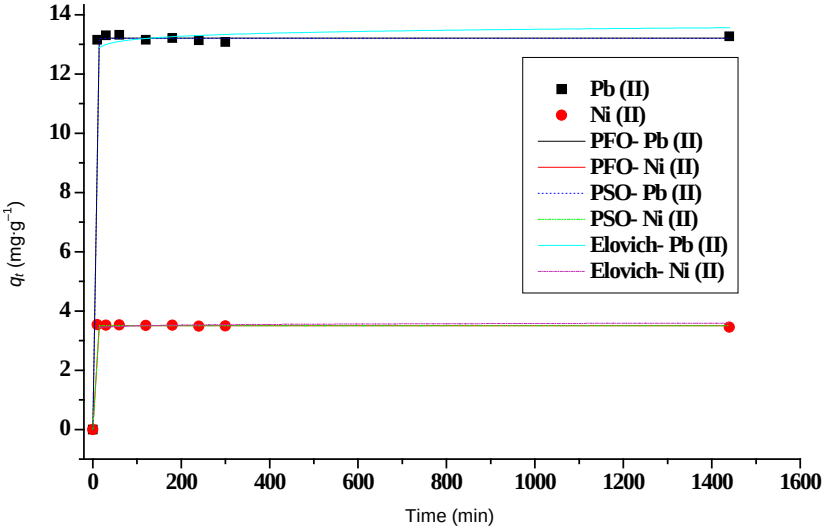

Fig. 7. Adsorption kinetics for lead-corn cob system; q_t = absorption capacity at time t, PFO = pseudo-first order, PSO = pseudo-second order; source: own study

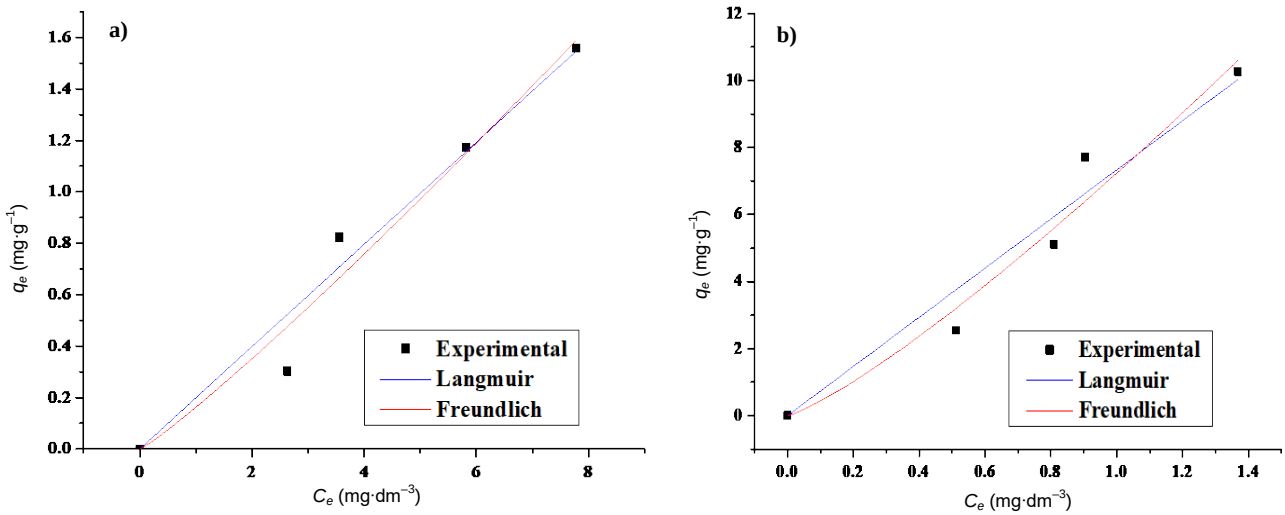

Fig. 8. Adsorption isotherms of investigated heavy metals on corn cob obtained by non-linear regression: a) Ni(II), b) Pb(II); C_e = concentration at the equilibrium, q_e = adsorption capacity at the equilibrium; source: own study

Table 7. Fitting parameters of nickel(II) and lead(II) adsorption isothermal models

Model	Parameter	Ni(II)	Pb(II)
Langmuir	q_{max} (mg·g^{-1})	1.5941	4.9944
	K_L (dm^3·g^{-1})	1248.6	14700.5
	R^2	0.9481	0.9350
Freundlich	K_F (mg·g^{-1}) (dm^3·mg^{-1})$^{1.0821}$	0.162	7.240
	n	0.899	0.821
	1/n	1.1123	1.2180
	R^2	0.9532	0.9489

Explanations: q_{max} = maximum adsorption capacity, K_L = ratio of the adsorption/desorption rate, R^2 = determination coefficient, K_F = parameter related to the affinity of the bioadsorbent for metal ions, n = parameter related to adsorption intensity.
Source: own study.

have an effect on the adsorption process and that the process occurs on the heterogeneous outer surface of the biomass.

ADSORPTION THERMODYNAMIC

The thermodynamic consideration of the adsorption process is essential to decide whether the process is feasible or not, exothermic or endothermic. The van't Hoff equation was used to calculate the values of $\Delta H°$, $\Delta G°$, and $\Delta S°$. The thermodynamic absorption parameters of Ni(II) and Pb(II) are reported in Table 8; enthalpy was found to have negative values for the removal of both metals, which indicates the exothermic character of the system. This is consistent with the increased removal of Pb(II) and Ni(II)

Table 8. Thermodynamic parameters

Temperature (°C)	Ni (II)			Pb (II)		
	$\Delta H°$	$\Delta S°$	$\Delta G°$	$\Delta H°$	$\Delta S°$	$\Delta G°$
	(KJ·mol^{-1})					
306.9	–7.4995	–0.05312	8.7995	–4.0653	–0.0259	3.8912
328.2	–	–	9.9309	–	–	4.4435
349.4	–	–	11.0570	–	–	4.9932

Explanations: $\Delta H°$ = standard enthalpy, $\Delta S°$ = standard entropy, $\Delta G°$ = Gibbs' standard free energy.
Source: own study.

as temperature increases. Furthermore, the negative value of the adsorption entropy shows that the process presents a modification in the surface of the adsorbent, so reversibility is little possible [DOBROSZ-GÓMEZ *et al.* 2018]. The positive values of Gibbs' energy prove that the system is not spontaneous, so it is necessary to provide energy to the system [HAROON *et al.* 2016].

CONCLUSIONS

It was found that the hydroxyl, carboxyl, and phenolic groups are the major contributors to the removal process and that Pb(II) forms coordination micro-complexes on the surface of the biomaterial, while Ni(II) forms bonds with the active centers. The best Ni(II) removal yields are achieved with 0.02 g of adsorbent and 70°C, while Pb(II) at 0.003 g and 55°C. The maximum Ni(II) adsorption capacity of 3.52 mg·g^{-1} (86%) and 13.32 mg·g^{-1} (94.3%) for Pb(II) was achieved at 250 and 330 min, respectively. Pseudo-first order and pseudo-second order models fit the data best, and Langmuir's and Freundlich's models describe the isotherm of the process. Thermodynamic parameters ($\Delta H°$, $\Delta G°$, $\Delta S°$) suggest that the adsorption process of both cations is exothermic, irreversible, and not spontaneous.

REFERENCES

ABDUL-HAMEED H.M., AL JUBOURY M.F. 2020. MgFe-doubled layers hydroxide intercalated with low cost local adsorbent using for removal of lead from aqueous solution. Journal of Water and Land Development. No. 45 (IV–VI) p. 10–18. DOI 10.24425/jwld.2020.133041.

BABAZADEH R., RAZMI J., PISHVAEE M.S, RABBANI M. 2017. A sustainable second-generation biodiesel supply chain network design problem under risk. Omega. Vol. 66 p. 258–277. DOI 10.1016/J.OMEGA.2015.12.010.

BARDESTANI R., ROY C., KALIAGUINE S. 2019. The effect of biochar mild air oxidation on the optimization of lead(II) adsorption from wastewater. Journal of Environmental Management. Vol. 240 p. 404–420. DOI 10.1016/j.jenvman.2019.03.110.

BUREVSKA K., MEMEDI H., LISICHKOV K., KUVENDZIEV S., MARINKOVSKI M., RUSESKA G., GROZDANOV A. 2017. Biosorption of nickel ions from aqueous solutions by natural and modified peanut husks: Equilibrium and kinetics. Water and Environment Journal. Promoting Sustainable Solutions. Vol. 32. Iss. 2 p. 276–284. DOI 10.1111/wej.12325.

CHEN Y., WANG H., ZHAO W., HUANG S. 2018. Four different kinds of peels as adsorbents for the removal of Cd (II) from aqueous solution: Kinetics, isotherm and mechanism. Journal of the Taiwan Institute of Chemical Engineers. Vol. 88. p. 146–151. DOI 10.1016/j.jtice.2018.03.046.

CHERIK D., LOUHAB K. 2018. A kinetics, isotherms, and thermodynamic study of Diclofenac adsorption using activated carbon prepared from olive stones. Journal of Dispersion Science and Technology. Vol. 39. No. 6 p. 814–825. DOI 10.1080/01932691.2017.1395346.

DAI Y., SUN ., WANG W., LU L., LIU M., LI J., ... ZHANG Y. 2018. Utilizations of agricultural waste as adsorbent for the removal of contaminants: A review. Chemosphere. Vol. 211 p. 235–253. DOI 10.1016/j.chemosphere.2018.06.179.

DOBROSZ-GÓMEZ I., GÓMEZ M., SANTA C. 2018. Optimización del proceso de adsorción de Cr(VI) sobre carbón activado de origen bituminoso [Optimization of the Cr(VI) adsorption process on activated carbon of bituminous origin]. Información Tecnológica. Vol. 29. No. 6 p. 43–56. DOI 10.4067/S0718-07642018000600043.

GAŁCZYŃSKA M., MAŃKOWSKA N., MILKE J., BUŚKO M. 2019. Possibilities and limitations of using *Lemna minor*, *Hydrocharis morsus-ranae* and *Ceratophyllum demersum* in removing metals with contaminated water. Journal of Water and Land Development. No. 40 p. 161–173. DOI 10.2478/jwld-2019-0018.

HAROON H., ASHFAQ T., GARDAZI S.M.H., SHERAZI T.A., ALI M., RASHID N., BILAL M. 2016. Equilibrium kinetic and thermodynamic studies of Cr(VI) adsorption onto a novel adsorbent of *Eucalyptus camaldulensis* waste: Batch and column reactors. Korean Journal of Chemical Engineering. Vol. 33 No. 10 p. 2898–2907. DOI 10.1007/s11814-016-0160-0.

HERNÁNDEZ RODIGUEZ M., YPERMAN J., CARLEER R., MAGGEN J., DADDI D., GRYGLEWICZ G., VAN DER BRUGGEN B., FALCÓN HERNÁNDEZ J., OTERO CALVIS A. 2018. Adsorption of Ni(II) on spent coffee and coffee husk based activated carbon. Journal of Environmental Chemical Engineering. Vol. 6. No. 1 p. 1161–1170. DOI 10.1016/j.jece.2017.12.045.

IBISI N.E., ASOLUKA C.A. 2018. Use of agro-waste (*Musa paradisiaca* peels) as a sustainable biosorbent for toxic metal ions removal from contaminated water. Chemistry International. Vol. 4. No. 1 p. 52–59.

JOHARI K., SAMAN N., SONG S.T., CHIN C.S., KONG H., MAT H. 2016. Adsorption enhancement of elemental mercury by various surface modified coconut husk as eco-friendly low-cost adsorbents. International Biodeterioration and Biodegradation Vol. 109 p. 45–52. DOI 10.1016/j.ibiod. 2016.01.004.

KAPLAN INCE O., INCE M., YONTEN V., GOKSU A. 2017. A food waste utilization study for removing lead(II) from drinks. Food Chemistry. Vol. 214 p. 637–643. DOI 10.1016/j.foodchem.2016.07.117.

LIU Z., DENG X., WANG M., CHEN J., ZHANG A., GU Z., ZHAO C. 2009. BSA-modified polyethersulfone membrane: Preparation, characterization and biocompatibility. Journal of Biomaterials Science, Polymer Edition. DOI 10.1163/156856209X412227.

MANIRETHAN V., GUPTA N., BALAKRISHNAN R.M., RAVAL K. 2019. Batch and continuous studies on the removal of heavy metals from aqueous solution using biosynthesised melanin-coated PVDF membranes. Environmental Science and Pollution Research. Vol. 27 p. 24723–24737. DOI 10.1007/s11356-019-06310-8.

MANJULADEVI M., ANITHA R., MANONMANI S. 2018. Kinetic study on adsorption of Cr(VI), Ni(II), Cd(II) and Pb(II) ions from aqueous solutions using activated carbon prepared from *Cucumis melo* peel. Applied Water Science. Vol. 8 No. 1 p. 36. DOI 10.1007/s13201-018-0674-1.

NASEEM K., HUMA R., SHAHBAZ A., JAMAL J., ZIA UR REHMAN M., SHARIF A., …, FAROOQI Z.H. 2019. Extraction of heavy metals from aqueous medium by husk biomass: Adsorption isotherm, kinetic and thermodynamic study. Zeitschrift für Physikalische Chemie. Vol. 233 Iss. 2 p. 201–223. DOI 10.1515/zpch-2018-1182.

OUHIMMOU M., RÖNNQVIST M., LAPOINTE L.-A. 2019. Assessment of sustainable integration of new products into value chain through a generic decision support model: An application to the forest value chain. Omega. Vol. 99, 102173. DOI 10.1016/J.OMEGA.2019.102173.

PRADHAN P., ARORA A., MAHAJANI S.M. 2018. Pilot scale evaluation of fuel pellets production from garden waste biomass. Energy for Sustainable Development. Vol. 43 p. 1–14. DOI 10.1016/j.esd.2017.11.005.

RAVAL N.P, SHAH P.U., SHAH N.K. 2016. Adsorptive removal of nickel(II) ions from aqueous environment: A review. Journal of Environmental Management. Vol. 179 p. 1–20. DOI 10.1016/j.jenvman.2016.04.045.

SHEN Z., ZHANG Y., MCMILLAN O., JIN F, AL-TABBAA A. 2017. Characteristics and mechanisms of nickel adsorption on biochars produced from wheat straw pellets and rice husk. Environmental Science and Pollution Research International. Vol. 24. No. 14 p. 12809–12819.

SINGH S., SHUKLA S. 2017. Theoretical studies on adsorption of Ni(II) from aqueous solution using *Citrus limetta* peels. Environmental Progress & Sustainable Energy. Vol. 36. No. 3 p. 864–872.

SIREGAR A., SULISTYO I., PRAYOGO N.A. 2020. Heavy metal contamination in water, sediments and *Planiliza subviridis* tissue in the Donan River, Indonesia. Journal of Water and Land Development. Vol. 45 (IV–VI) p. 157–164. DOI 10.24425/jwld.2020.133057.

TEJADA-TOVAR C., GONZALEZ-DELGADO A., VILLABONA-ORTIZ A. 2019a. Characterization of residual biomasses and its application for the removal of lead ions from aqueous solution. Applied Sciences. Vol. 9. No. 21, 4486. DOI 10.3390/app9214486.

TEJADA-TOVAR C., VILLABONA-ORTÍZ A., GONZÁLEZ-DELGADO Á.D., GRANADOS-CONDE C., JIMÉNEZ-VILLADIEGO M. 2019b. Kinetics of mercury and nickel adsorption using chemically pretreated cocoa (*Theobroma cacao*) husk. Transactions of the ASABE. Vol. 62. No. 2 p. 461–466. DOI 10.13031/trans.13133.

VALENCIA J.A.R., GONZÁLEZ J.P., JIMENEZ-PITRE I., MOLINA-BOLÍVAR G. 2019. Physico-chemical treatment of waste water contaminated with heavy metals in the industry of metallic coatings. Journal of Water and Land Development. Vol. 43 p. 171–176. DOI 10.2478/jwld-2019-0075.

YI Y., LV J., LIU Y., WU G. 2017. Synthesis and application of modified litchi peel for removal of hexavalent chromium from aqueous solutions. Journal of Molecular Liquids. Vol. 225 p. 28–33. DOI 10.1016/j.molliq.2016.10.140.

YIN W., ZHAO C., XU J., ZHANG J., GUO Z., SHAO Y. 2019. Removal of Cd(II) and Ni(II) from aqueous solutions using activated carbon developed from powder-hydrolyzed-feathers and *Trapa natans* husks. Colloids and Surfaces A: Physicochemical and Engineering Aspects. Vol. 560 p. 426–433. DOI 10.1016/j.colsurfa.2018.10.031.